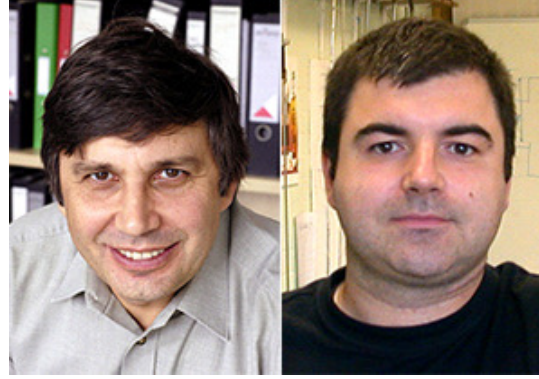
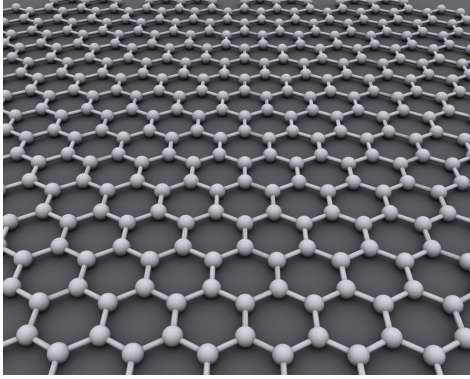


- 1. Introduction:
Fast photodetectors. Why graphene based?
- 2. Photothermoelectric graphene based detectors.
- 3. THz detection using photo thermoelectric effect in graphene.
- 4. Ultrafast graphene photodetectors
- 5. Conclusions



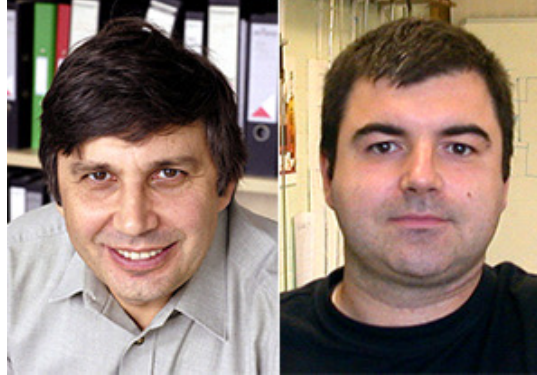
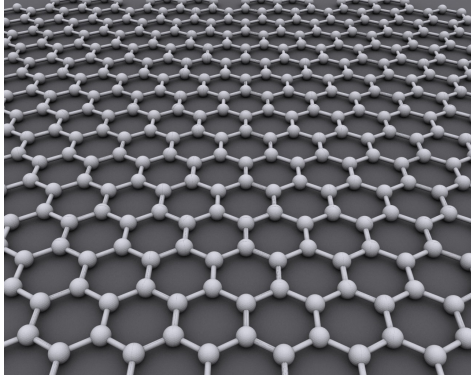
Nobel Prize in Physics 2010



Graphene Flagship Technology and Innovation Roadmap



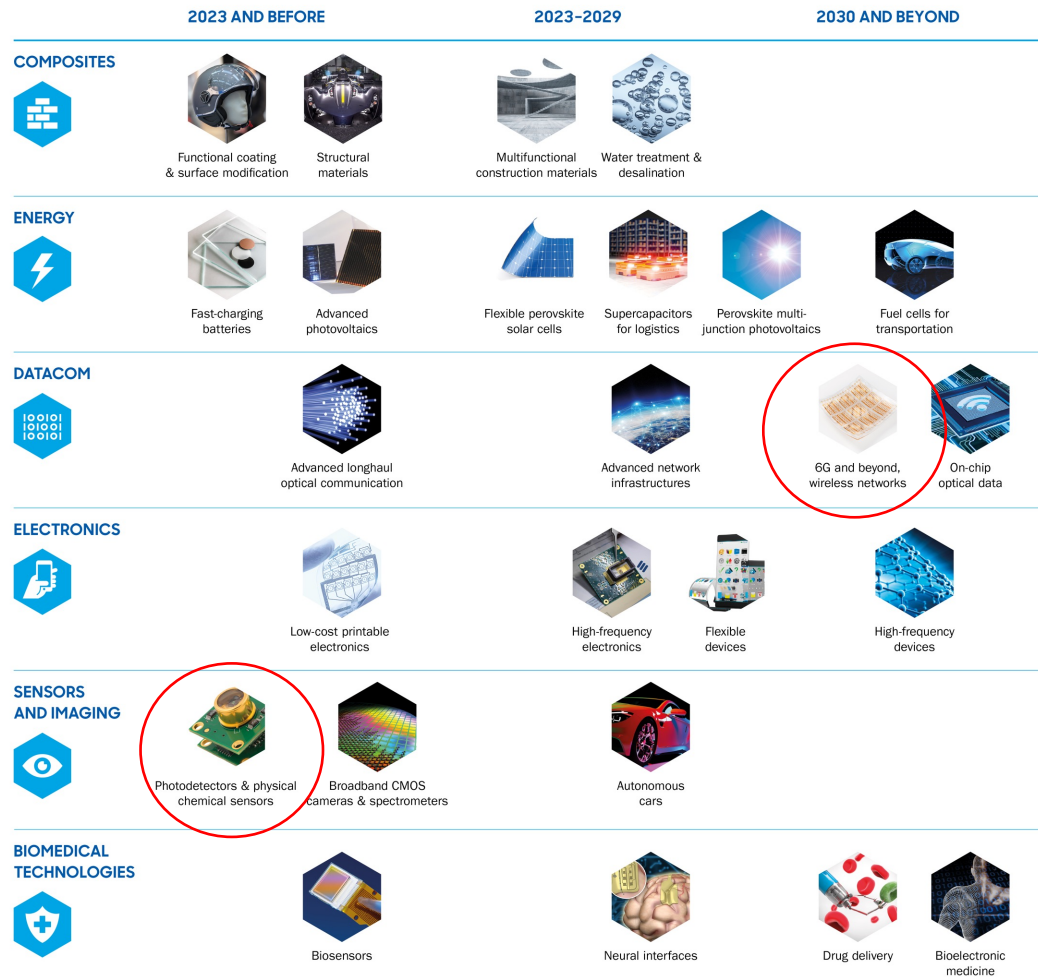
Funded by the European Union



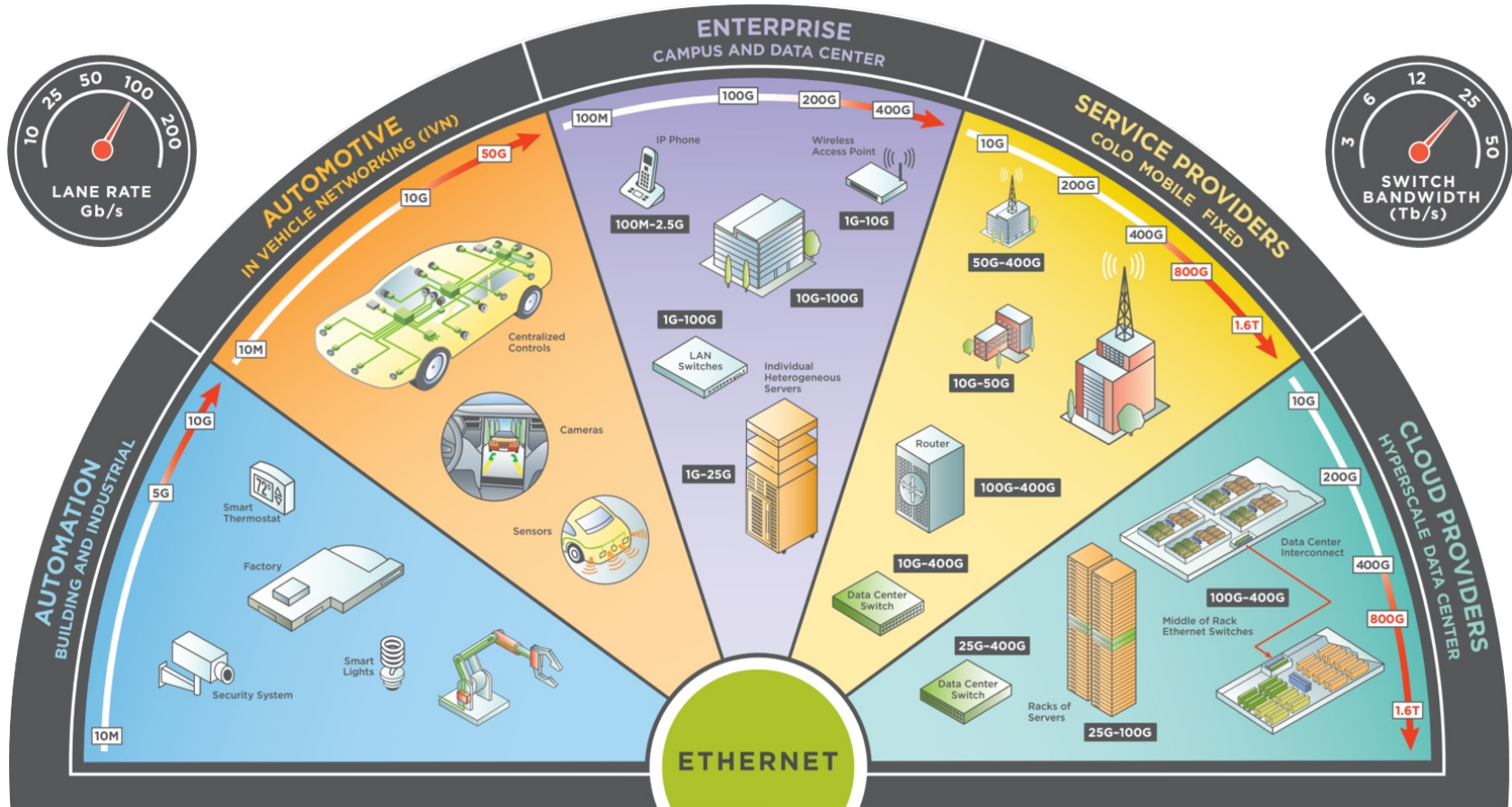
Nobel Prize in Physics 2010



Graphene Flagship Technology and Innovation Roadmap

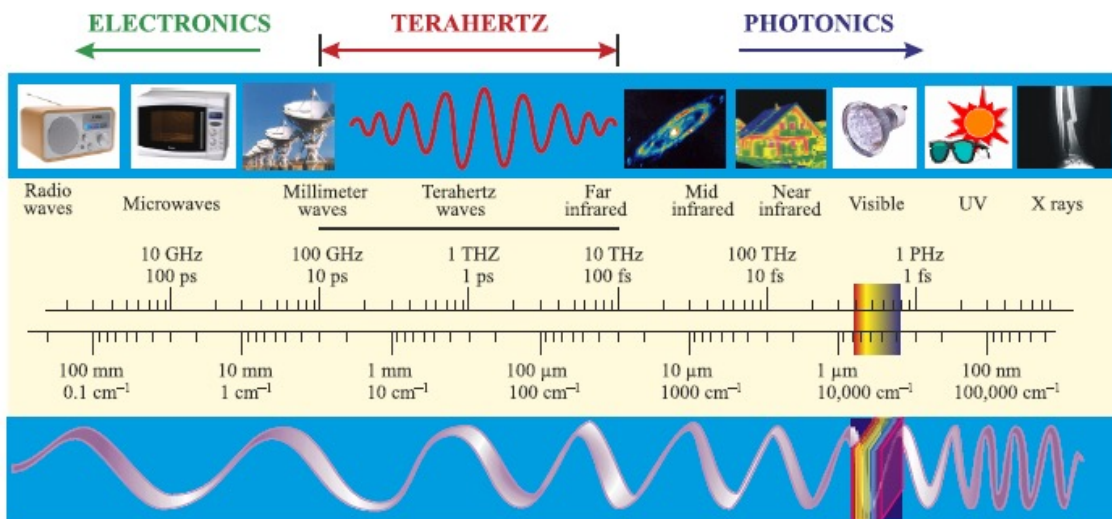


Motivation



The main limiting factors for development of new generation telecommunication systems is the lack of hardware components, in particular, cheap, sensitive and high-speed photodetectors operating at room temperature.

Motivation



Detectors.

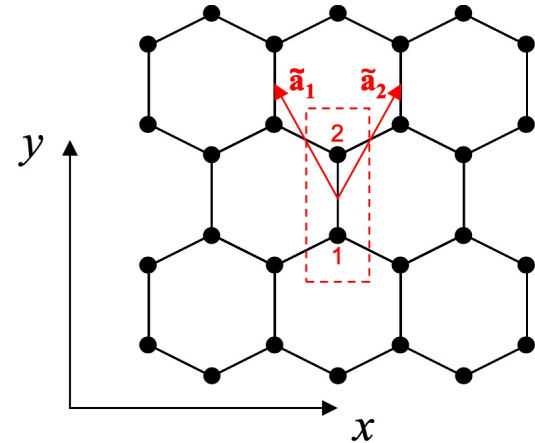
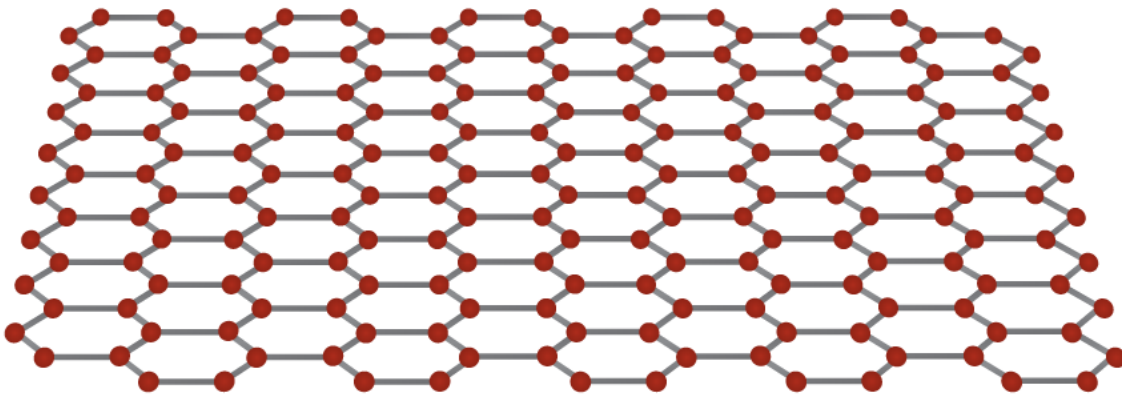
Why nanosturture:

- Sensitive
- Fast
- Energy efficient
- Spectral sensitive

Detectors. Why graphene (CNT) based:

- Gapless graphene has strong interband absorption at all frequencies
- High room-temperature mobility
- Geometric control of the band structure
- Easy to fabricate

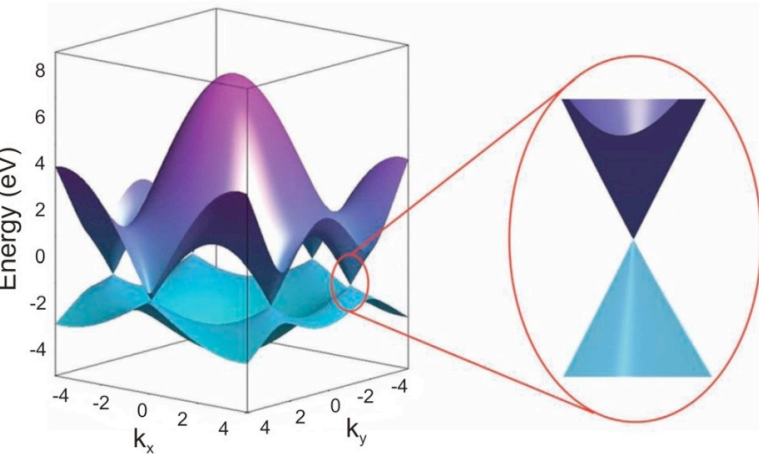
Motivation



Detectors. Why graphene (CNT) based:

- Gapless graphene has strong interband absorption at all frequencies
- High room-temperature mobility
- Geometric control of the band structure
 - Easy to fabricate

Motivation



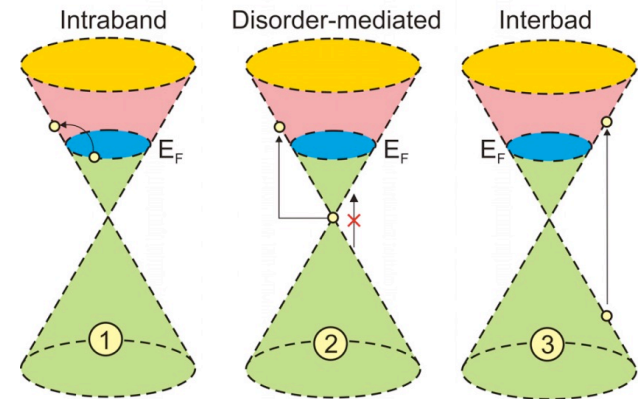
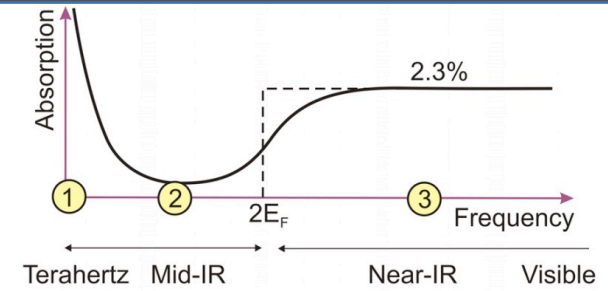
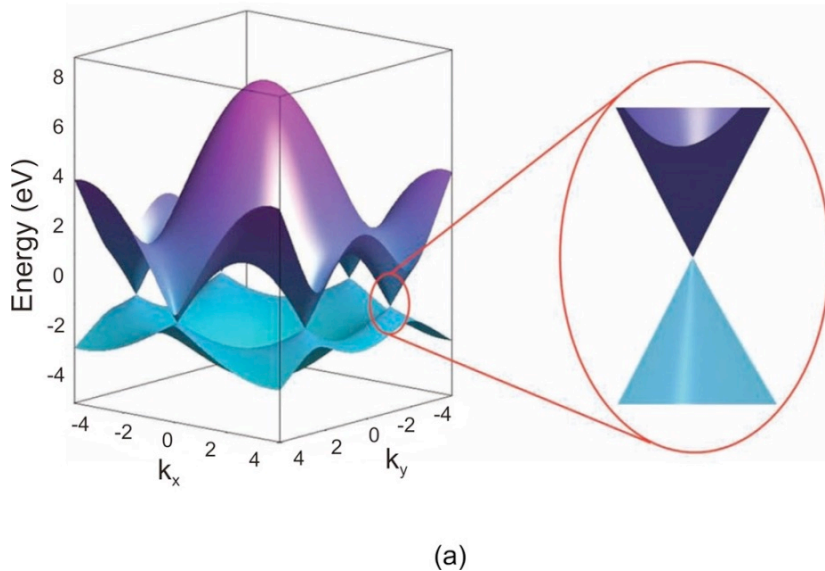
(a)

$$E(k) = E_0 + 2\gamma_1 \left(\cos(\vec{k}\vec{a}_1) + \cos(\vec{k}\vec{a}_2) + \cos(\vec{k}(\vec{a}_1 - \vec{a}_2)) \right) \\ \pm \gamma_0 \sqrt{3 + 2\cos\vec{k}\vec{a}_1 + 2\cos\vec{k}\vec{a}_2 + 2\cos\vec{k}(\vec{a}_1 - \vec{a}_2)}$$

Detectors. Why graphene (CNT) based:

- **Gapless graphene has strong interband absorption at all frequencies**
- **High room-temperature mobility**
- **Geometric control of the band structure**
 - **Easy to fabricate**

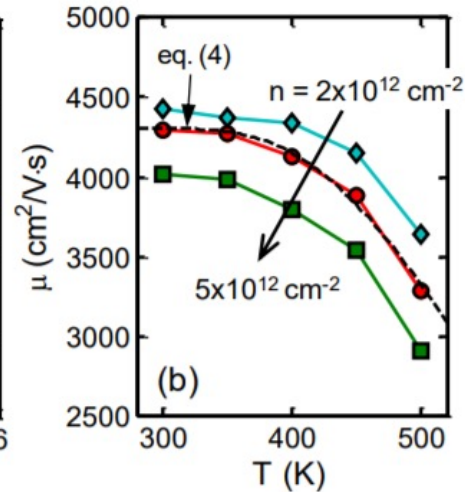
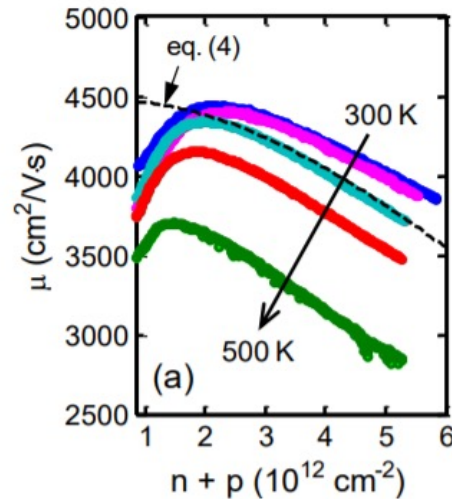
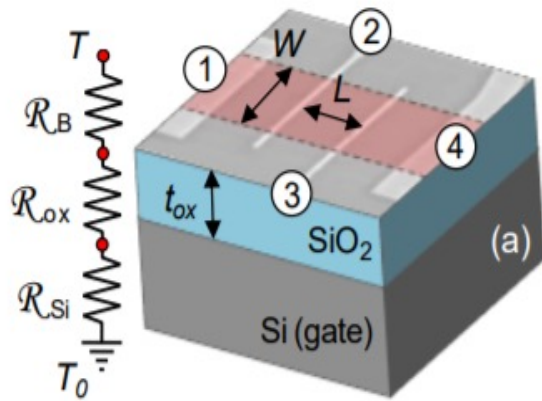
Motivation



Detectors. Why graphene (CNT) based:

- **Gapless graphene has strong interband absorption at all frequencies**
- **High room-temperature mobility**
- **Geometric control of the band structure**
 - **Easy to fabricate**

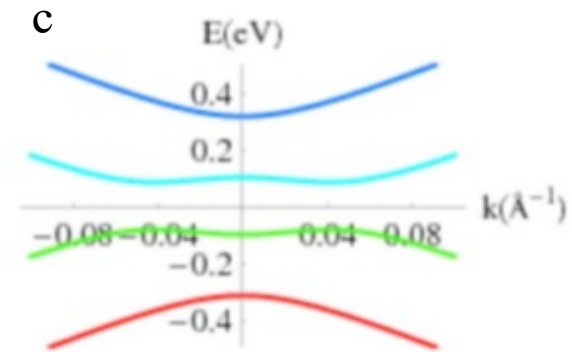
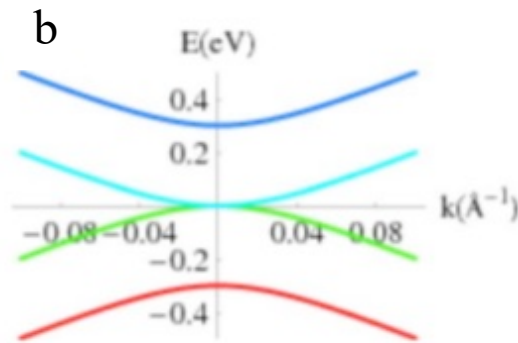
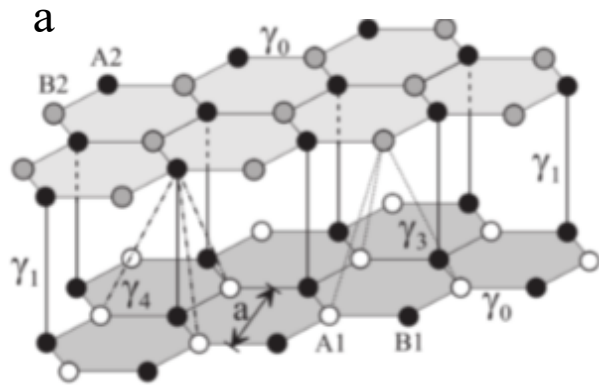
Motivation



Detectors. Why graphene (CNT) based:

- Gapless graphene has strong interband absorption at all frequencies
- High room-temperature mobility
- Geometric control of the band structure
 - Easy to fabricate

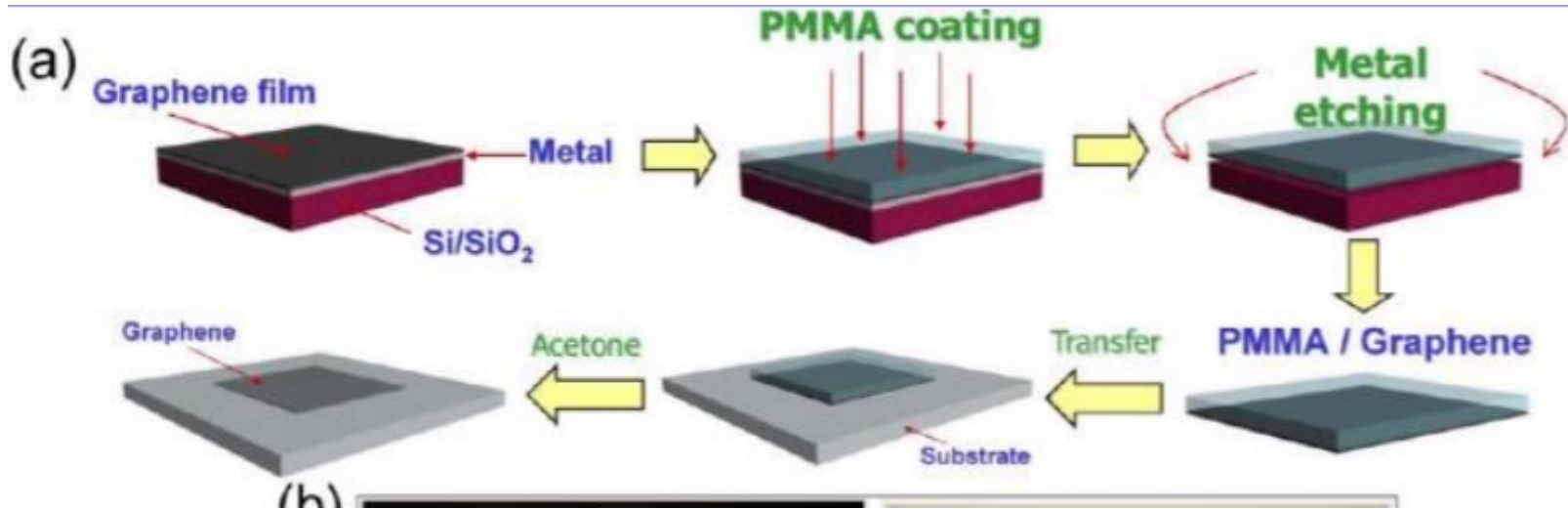
Motivation



Detectors. Why graphene (CNT) based:

- Gapless graphene has strong interband absorption at all frequencies
- High room-temperature mobility
- Geometric and electrostatic control of the band structure
- Easy to fabricate

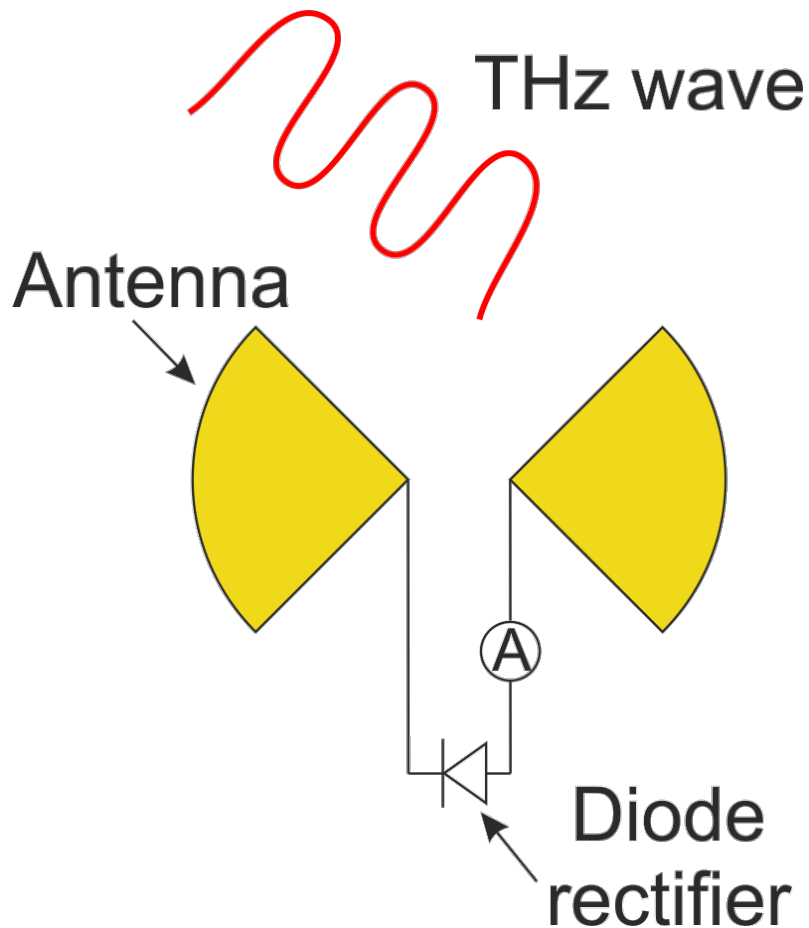
Motivation



Detectors. Why graphene (CNT) based:

- Gapless graphene has strong interband absorption at all frequencies
- High room-temperature mobility
- Geometric control of the band structure
 - **Easy to fabricate**

What do we mean by graphene THz detector



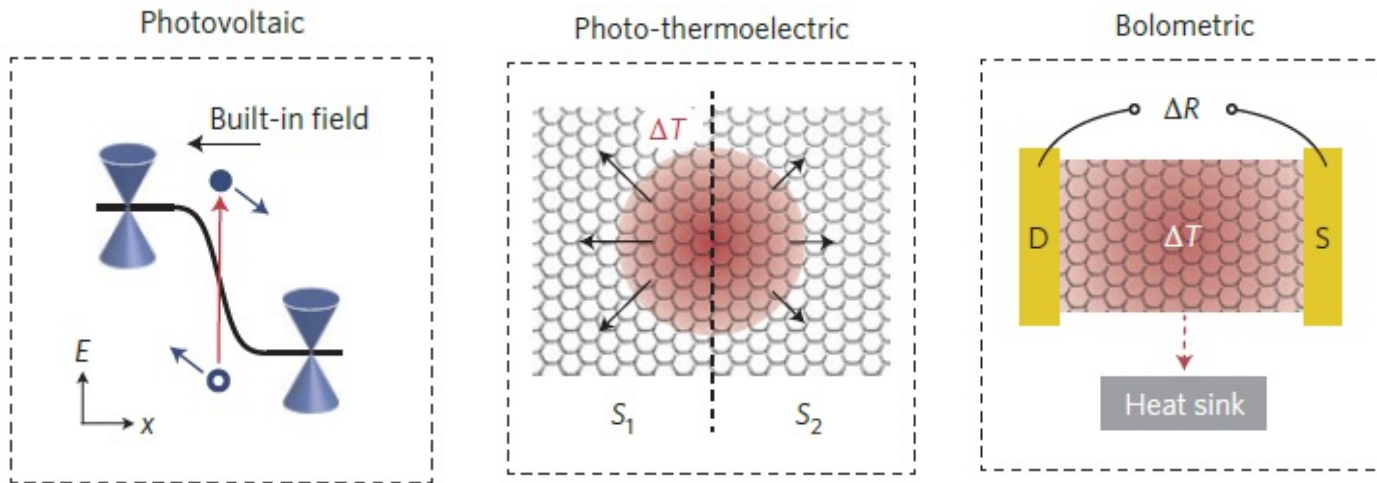
$$\langle I(\delta V \cos \omega t) \rangle_T \approx$$

$$\frac{dI}{dV} \delta V \langle \cos \omega t \rangle_T + \frac{1}{2} \frac{d^2 I}{dV^2} \delta V^2 \langle \cos^2 \omega t \rangle_T$$

$$= \frac{1}{4} \frac{d^2 I}{dV^2} \delta V^2$$

Study of detection mechanisms
is the study of nonlinearities

The main mechanisms of EM radiation detection by graphene-based devices



Current due to built-in field at the junction OR rectification due to diode nonlinearity

Voltage due to temperature gradients in nonuniformly doped channel

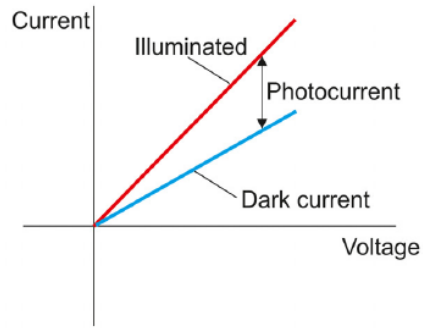
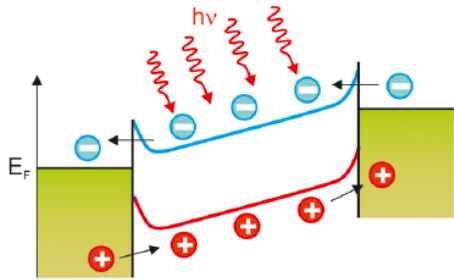
Resistance change due to overall device heating

Figure from: F.H.L. Koppens, T. Mueller, P. Avouris, A.C. Ferrari, M.S. Vitiello, M. Polini, "Photodetectors based on graphene, other two-dimensional materials and hybrid systems" *Nature nanotechnology*, 9, 780-793 (2014)

The main mechanisms of EM radiation detection by graphene-based devices

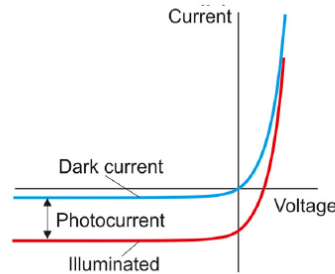
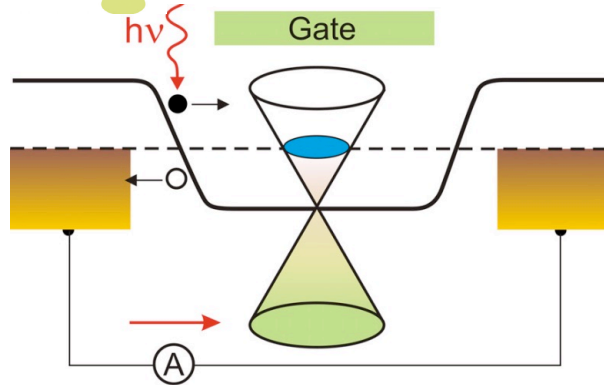
Graphene photodetectors

Bolometric detector



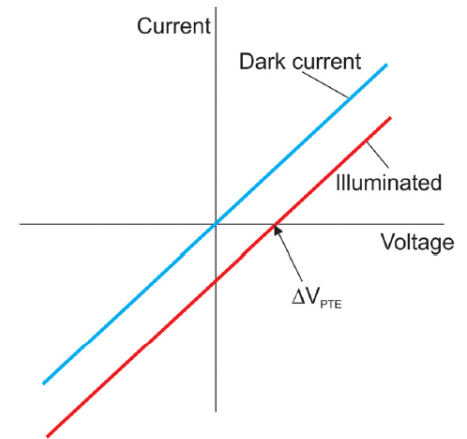
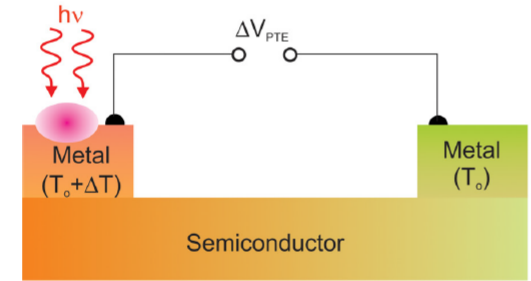
(a)

$$\Delta V = I_{dc} \Delta R = I_{dc} \frac{dR}{dT} \Delta T$$



(b)

Photo-thermoelectric detector



$$V_{PTE} = S \Delta T \quad S = -\frac{\pi^2 k_B^2 T}{3e} \left(\frac{d \ln \sigma}{dE} \right) \Big|_{E=E_F}$$

The main mechanisms of EM radiation detection by graphene-based devices

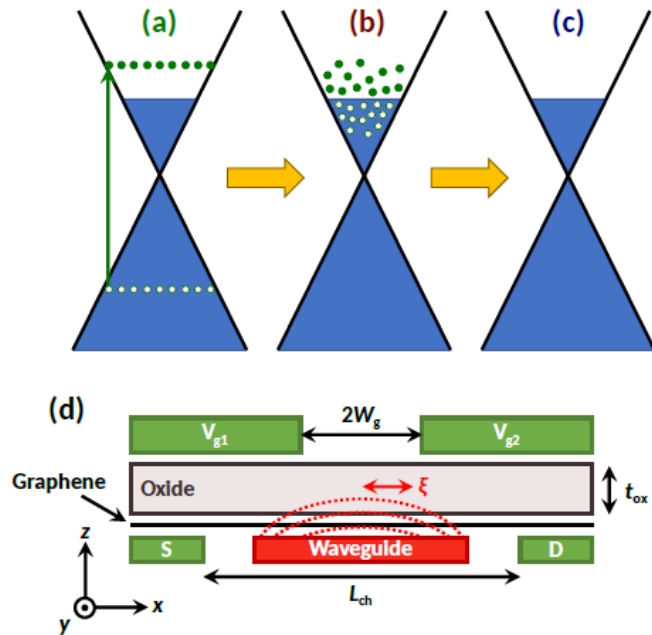


FIG. 1. Schematic of the photothermoelectric effect in graphene. (a) Optical absorption generates an excited population of electrons and holes, (b) interparticle scattering thermalizes photoexcited carriers to an elevated temperature, and (c) electron-phonon scattering relaxes the electron temperature back to the lattice temperature. Panel (d) shows a cross section of a graphene PTE detector, where split gates generate a pn junction in the graphene channel, resulting in a thermoelectric voltage between the source and drain contacts.

$$V_{\text{PTE}} = \int S(x) \frac{dT_{\text{el}}(x)}{dx} dx, \quad (1)$$

$$\vec{\nabla} \cdot [\kappa(x, y) \nabla T_{\text{el}}(x, y)] - \gamma(x, y) C_{\text{el}}(x, y) T_{\text{el}}(x, y) + P(x, y) = 0, \quad (4)$$

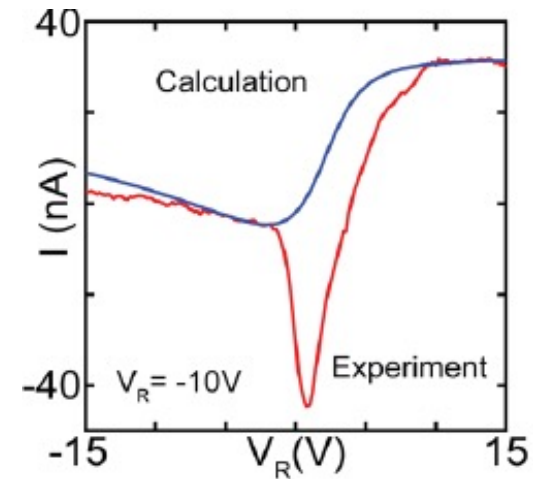
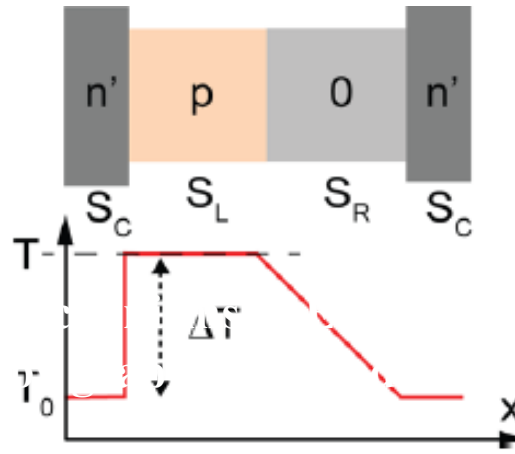
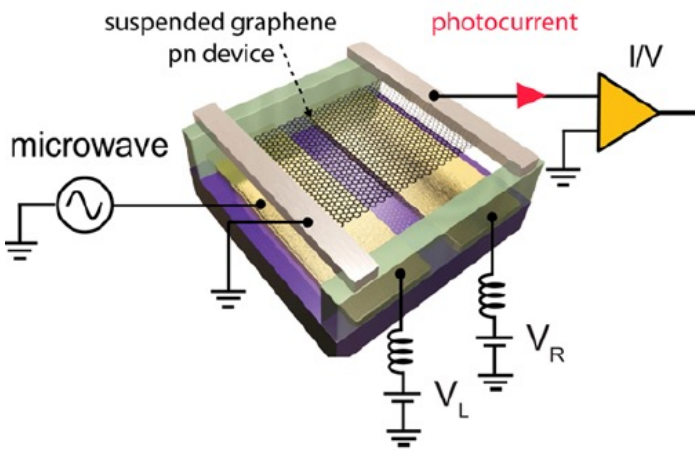
where the x -axis (y -axis) is parallel (perpendicular) to the graphene channel, $\kappa(x, y)$ is the electronic thermal conductivity, $\gamma(x, y)$ is the electron cooling rate, $C_{\text{el}}(x, y)$ is the electronic heat capacity, and $P(x, y)$ is the optical power density incident on the graphene sheet. We assume

$$P(x, y) = P_{\text{in}} \cdot G(x) \cdot \frac{1}{L_{\alpha}} e^{-y/L_{\alpha}}, \quad (5)$$

Antidormi, Aleandro, and Aron W. Cummings. "Optimizing the photothermoelectric effect in graphene." arXiv preprint arXiv:2102.11225 (2021).

Photo-thermoelectric effect in graphene

In case of a **photothermoelectric effect** an non-uniform doping of the channel and non-uniform heating of the channel results in onset of a DC voltage proportional to increase of the electron temperature



Graphene advantages for hot-electron photothermoelectric detection:

- Gapless graphene has strong interband absorption at all frequencies.
- The electronic heat capacity of single-layer graphene is much lower than in bulk materials, resulting in a larger change in temperature for the same absorbed energy
- The photothermoelectric effect has a picosecond response time, set by the electron– phonon relaxation rate

Photo-thermoelectric effect

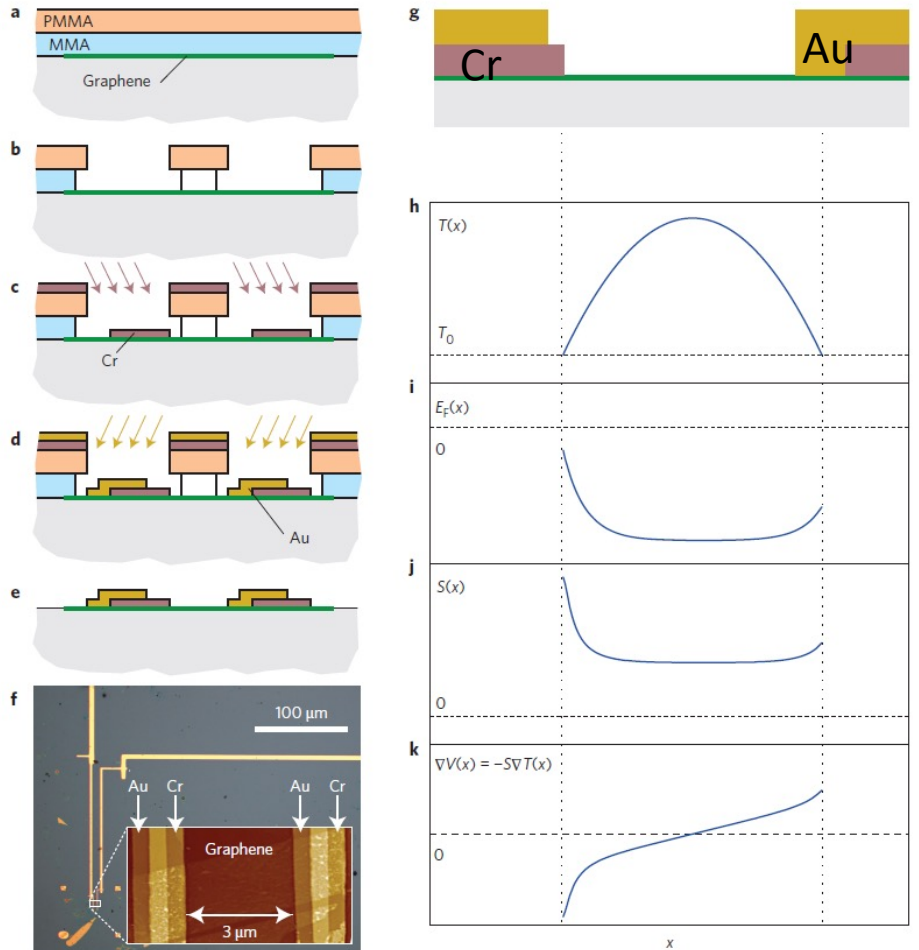
$$U_{PTE} = -\int SdT \approx S(T_S - T_D)$$

$$S \approx -\frac{\pi^2 k_B^2 T}{3e} \frac{1}{\sigma} \frac{d\sigma}{dE_F}$$

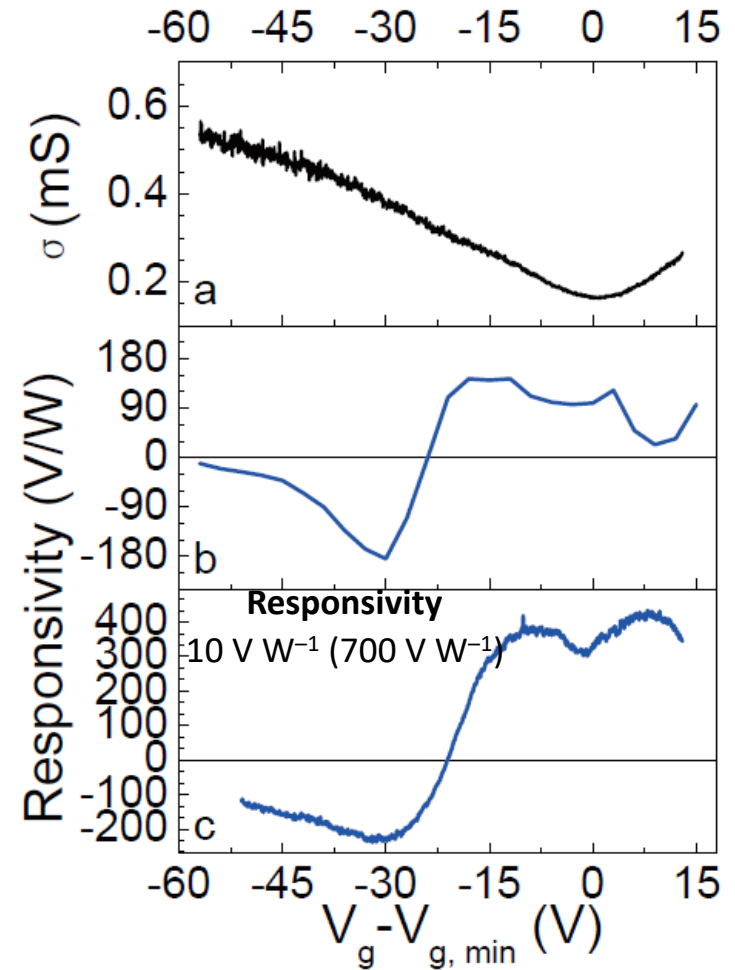
Photo-thermoelectric effect in graphene in THz region

Graphene photothermoelectric detector.

Principle of operation



Graphene photothermoelectric detector device fabrication and principle of operation. (a-e) Lithographic sequence used to produce the graphene terahertz detector. (f) Optical micrograph showing electrical contacts and (inset) atomic force micrograph showing bimetallic contacts connected to an exfoliated graphene layer. (g-k) Schematic of the principle components during device operation. (g) Cross-sectional view of the device. (h-j) Profiles across the device of (h) electron temperature $T(x)$, (i) Fermi level $E_F(x)$, (j) Seebeck coefficient $S(x)$ and (k) potential gradient



Broadband thermoelectric responsivity of graphene photothermoelectric detector. (a,d) Electrical conductance, (b,e) responsivity to Joule heating, and (c,f) responsivity to radiation as a function of gate voltage for the device shown in Fig. 1f at room temperature and in ambient environment.

Waveguide Integrated Graphene Photodetector*

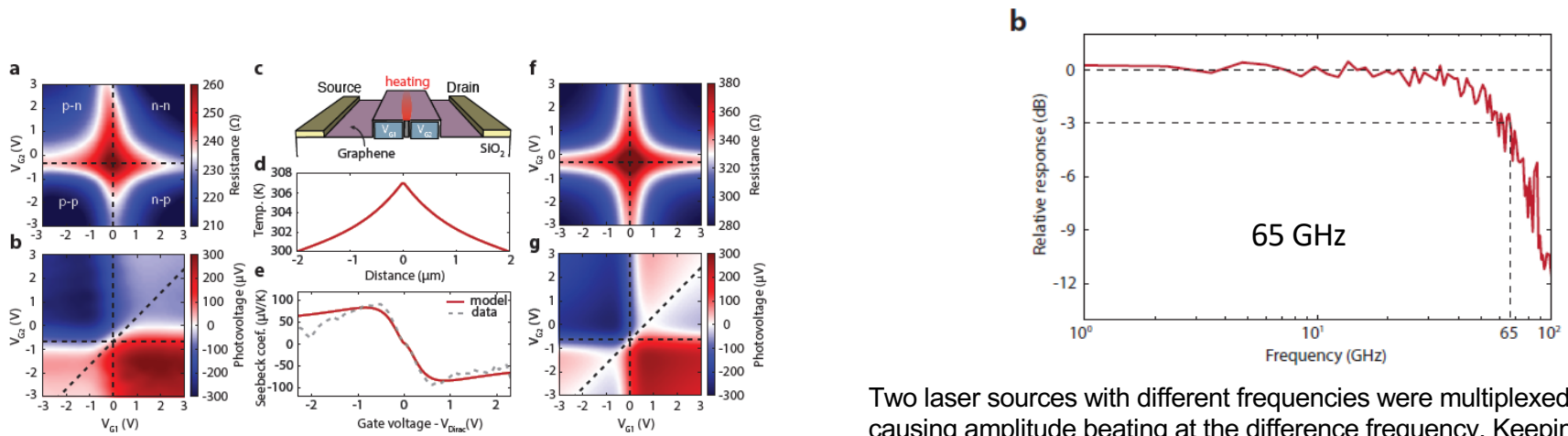


Figure 2. Results for Sample A. **(a)** Resistance map for varying gate voltages V_{G1} and V_{G2} applied to the slot-waveguide. Four characteristic regions can be identified; n-n, n-p, p-p and p-n, indicating the gate-tunability of the carriers. The resistance peak indicates the charge neutrality point (Dirac point) of the device. **(b)** Measured photovoltage map at zero bias. **(c)** Sketch of the modeled structure. **(d)** Calculated electron temperature profile over the distance between the source and drain contacts. **(e)** Seebeck coefficient as a function of gate voltage ($V_{G1} = V_{G2} = V_G$) as calculated from the model and the measured data, plotted as solid and dashed lines, respectively. **(f)** Calculated resistance map depending on the gate voltages. **(g)** Corresponding photovoltage map, calculated using the Mott formula. The measured and calculated photovoltage are in good agreement.

BD=65 GHz
Ra=35 mA/W

Two laser sources with different frequencies were multiplexed, causing amplitude beating at the difference frequency. Keeping the frequency of one laser constant while tuning the other, the difference frequency can be varied between 1 and 100 GHz. The laser light was amplified with an erbium-doped fiber amplifier and coupled into the graphene photodetector. A 67 GHz SG-probe was used to contact the device and the output power was detected with an RF power meter. A sketch of the measurement setup is depicted in the Supporting Information. The frequency response of the detector is shown in Figure 4(b). From this measurement we obtain a 3-dB cut-off frequency of ≈ 65 GHz, independent of bias voltage, which translates into a potential bit rate of ~ 90 Gbit/s (for a single wavelength channel and on-off keying), and is the highest value reported for a graphene photodetector. The maximum output power measured at 1 GHz was -31 dBm at 19.4 dBm optical input power and 1.2 V bias and defines the highest RF output power delivered by a graphene detector.

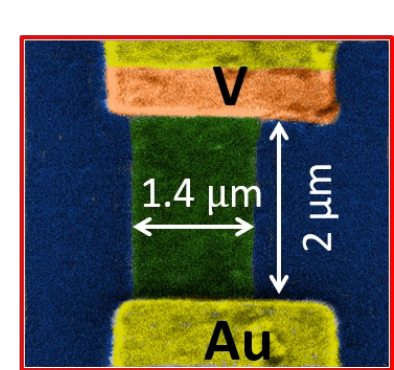
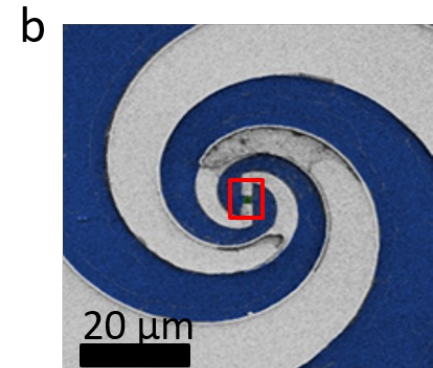
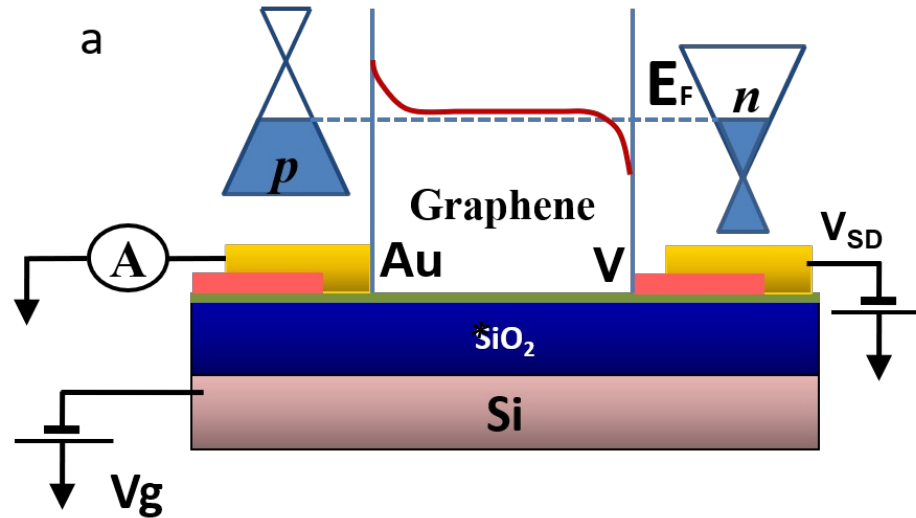
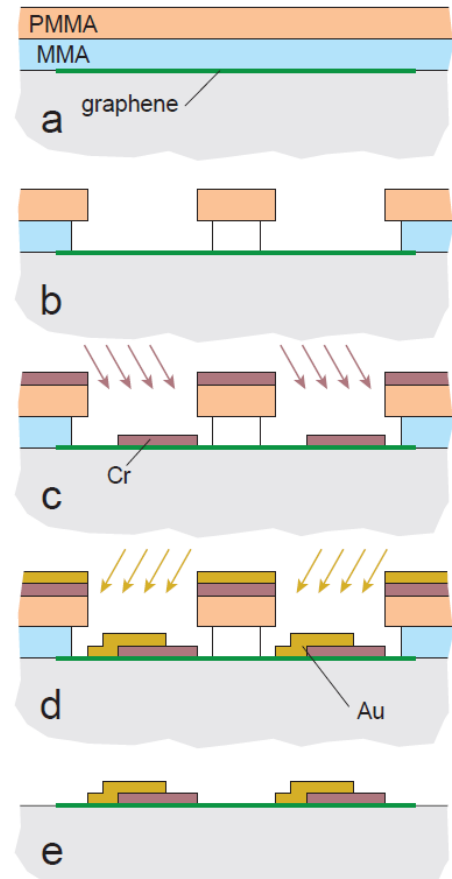
Overview of graphene based photodetectors*

Table 1. Comparison of WG-Integrated GPDs

ref	dominant mechanism	dark current (applied bias)	type of graphene	responsivity	bandwidth
this work	PTE	none	CVD	$R_V = 6 \text{ V W}^{-1}$	>67 GHz (setup-limited)
14	PV	none	CVD	$R_I = 0.016 \text{ A W}^{-1}$	41 GHz
15	PTE	none	flake	$R_V = 4.7 \text{ V W}^{-1}$	18 GHz
	PV/PBM at 0.4 V bias	0.4 V		$R_I = 0.17 \text{ A W}^{-1}$	(pulse measurement)
16	PBM	1 V	CVD	$R_I = 0.001 \text{ A W}^{-1}$ $R_V = 0.13 \text{ V W}^{-1}$	76 GHz
17	n/a	1 V 0.5 V	CVD	$R_I = 0.18 \text{ A W}^{-1}$ at 0.5 V bias $R_V = \text{V W}^{-1}$ at 0.5 V bias	>128 GHz at 1 V bias (setup-limited)
18	PBM	4 mA (0.4 V)	CVD	$R_I = 0.5 \text{ A W}^{-1}$	110 GHz
19	PV	1.6 V	CVD	0.36 A W^{-1}	110 GHz
23	PTE	none	flake	$R_I = 0.078 \text{ A W}^{-1}$ ($R_I = 0.36 \text{ A W}^{-1}$ at 1.2 V bias)	42 GHz
24	PTE	none	CVD	$R_V = 12 \text{ V W}^{-1}$	42 GHz
25	PTE	none	flake	$R_V = 3.5 \text{ V W}^{-1}$ $R_I = 0.035 \text{ A W}^{-1}$	65 GHz

*Mišeikis, Vaidotas, et al. "Ultrafast, zero-bias, graphene photodetectors with polymeric gate dielectric on passive photonic waveguides." *ACS nano* 14.9 (2020): 11190-11204.

Graphene based lateral Schottky diodes. Device fabrication



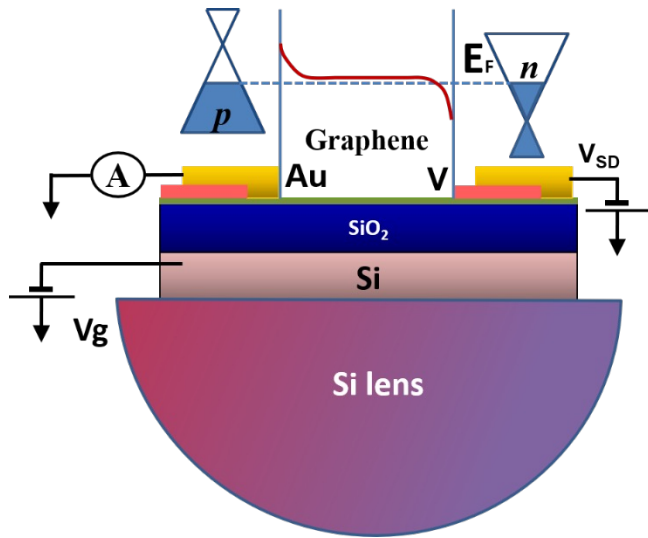
We use simple one-step lithography combined with shadow evaporation and lift-off in order to make asymmetric devices. Contact doping leads to formation of a p-n junction

The devices are coupled to the radiation with a logarithmic spiral antenna

5/23/24

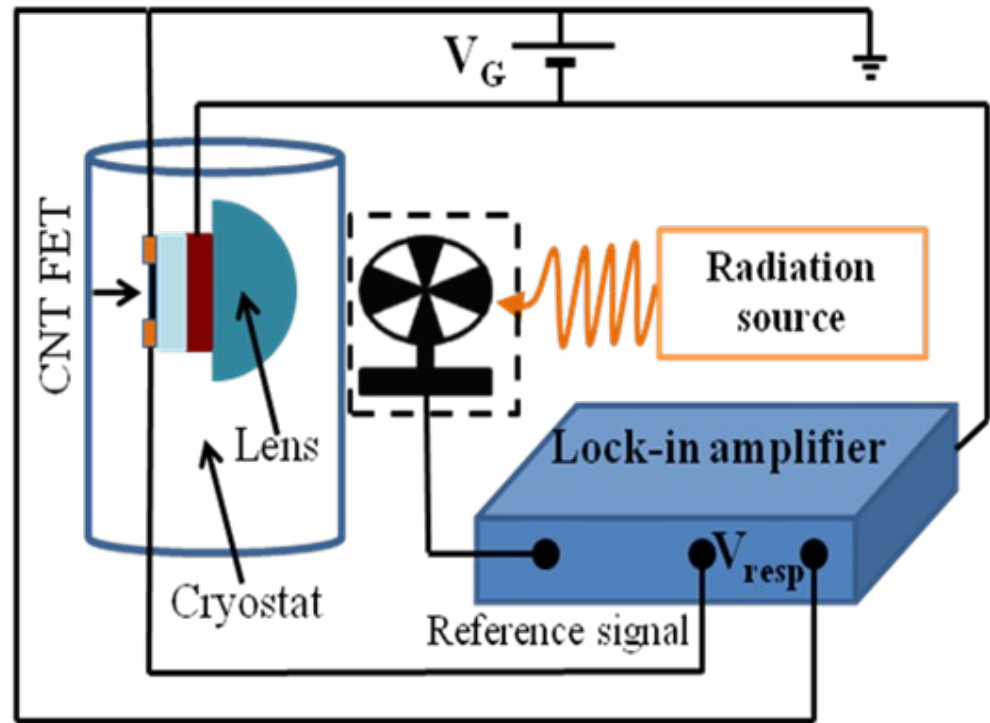
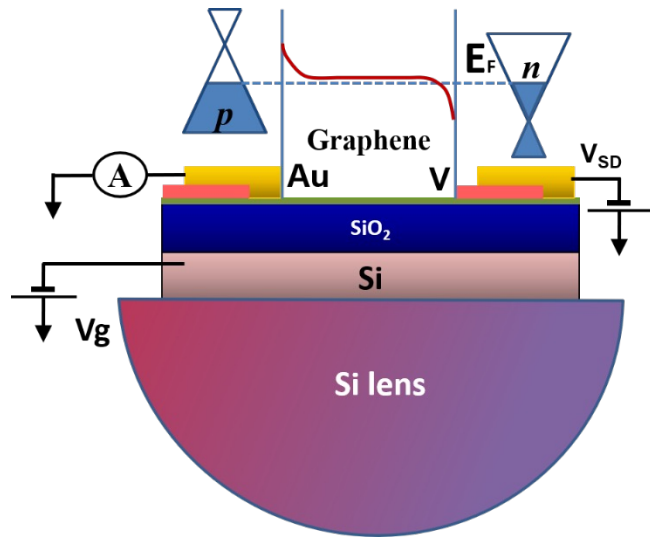
* Nature Nanotechnology **9**, 814–819 (2014)

Main approach: we compare many varieties using same setup



A device chip was fixed on a flat surface of a silicon lens and input inside the optical cryostat.,

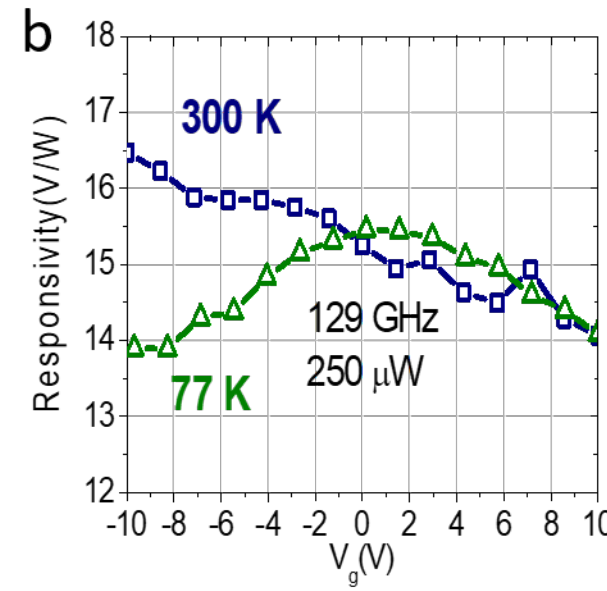
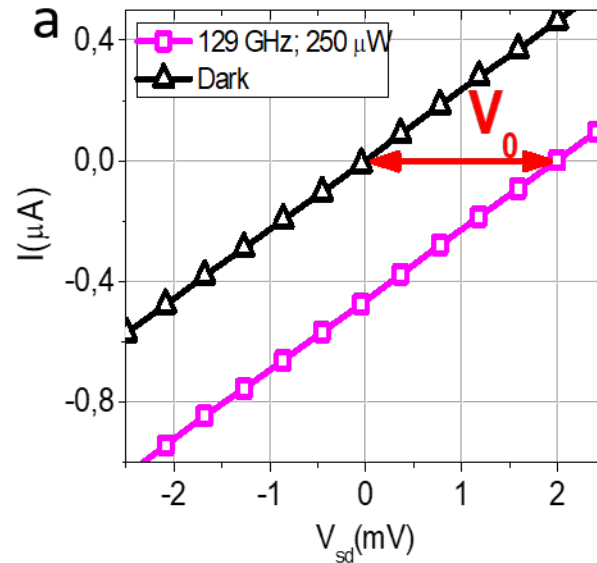
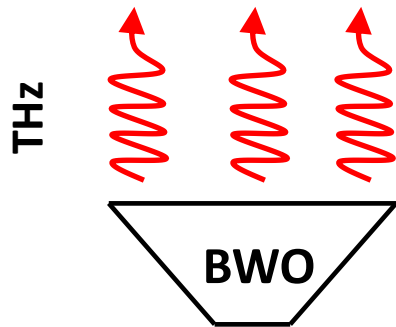
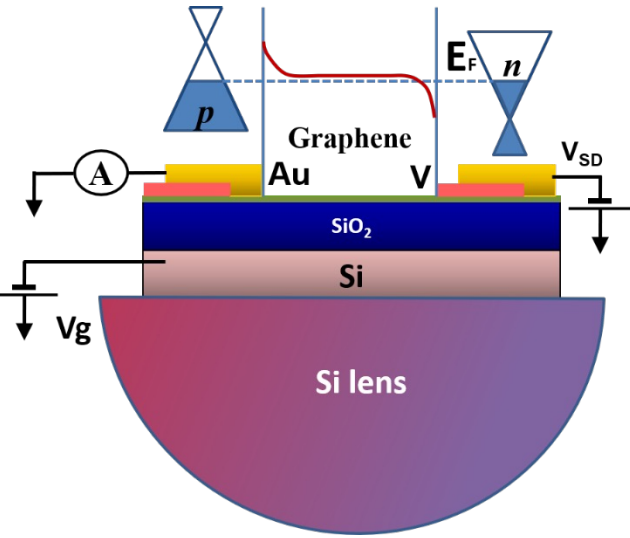
Main approach: we compare many varieties using same setup



A device chip was fixed on a flat surface of a silicon lens and input inside the optical cryostat.

The terahertz radiation provided by a two backward wave oscillators (140GHz, 250 to 450 GHz) and used a gas discharge laser operating on a 2.5 THz H₂O line.

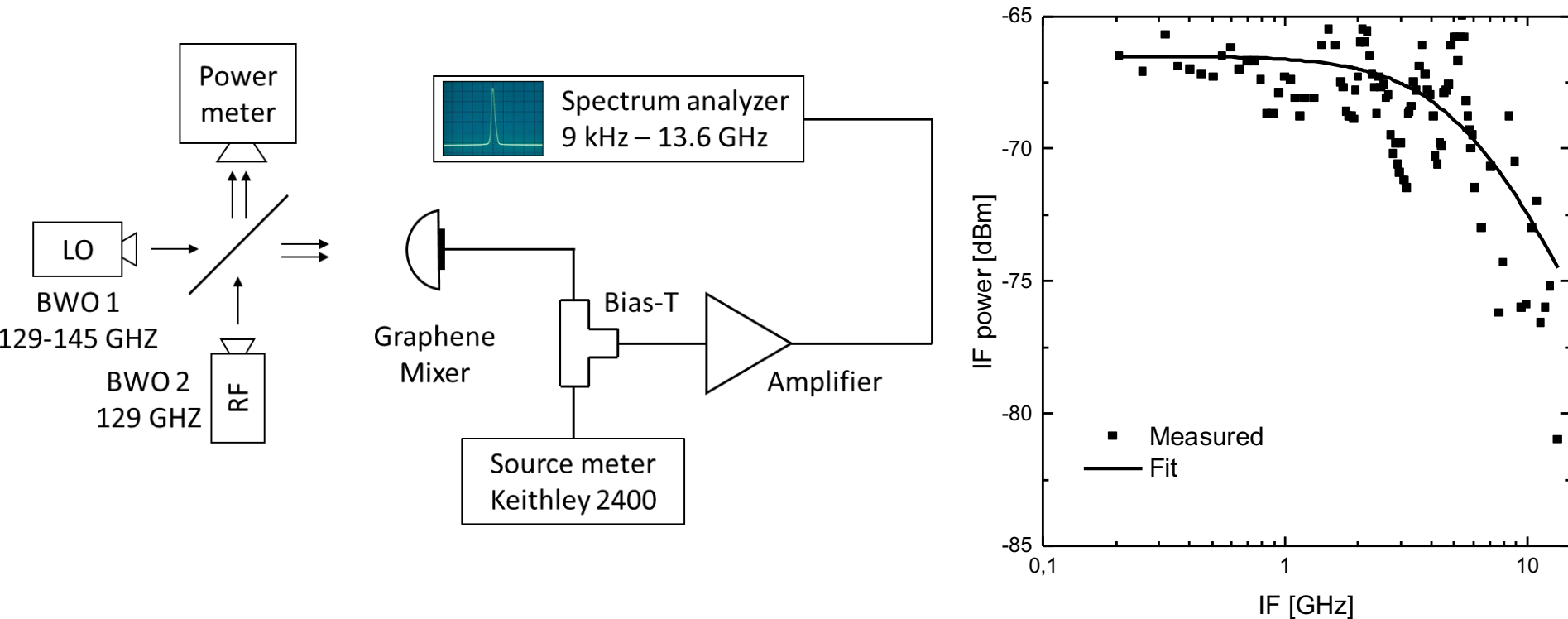
Graphene based THz detectors. Device characterization



When the device is exposed to 129 GHz radiation, with a power of $P = 250 \mu\text{W}$, the I-V curve shifts to the right. As shown, the zero-current crossing was shifted by a voltage V_0 of about 2 mV. This DC voltage V_0 induced by the radiation is the response voltage V_{RESP} .

Responsivity defined as V_{RESP}/P , where P is a power incident on the device with allowance for absorption in silicon

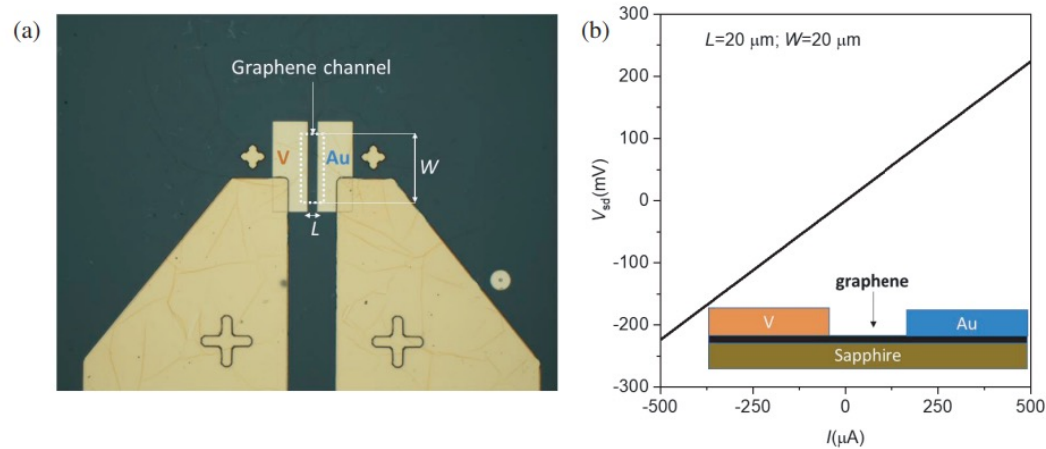
Graphene two terminal detector as THz mixer



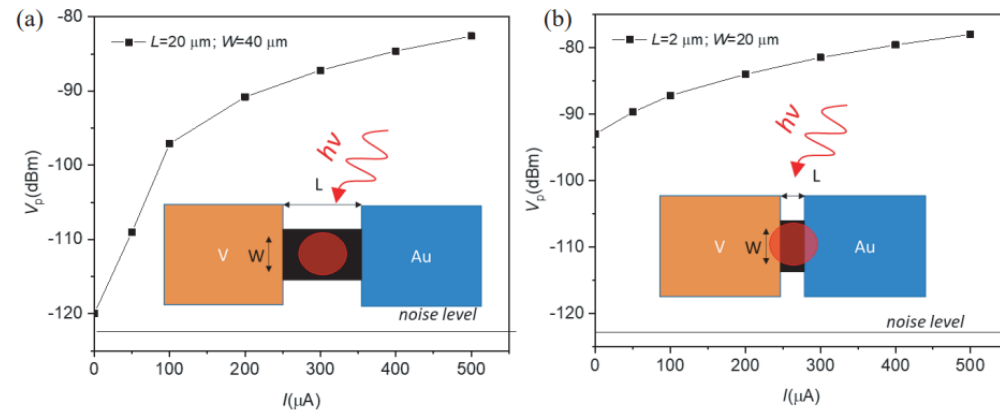
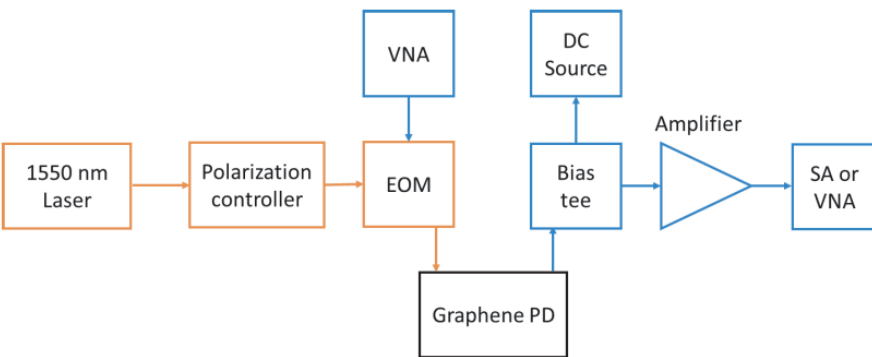
We have demonstrated that a two-terminal device based on graphene can be used as a THz radiation mixer with a **5.8 GHz bandwidth**. Our previous work on the direct detection of THz radiation with graphene detectors showed that the equivalent noise power of such detectors does not exceed **1 nW/Hz^{0.5}**.

Ultrafast photodetectors based on graphene

Device characterization



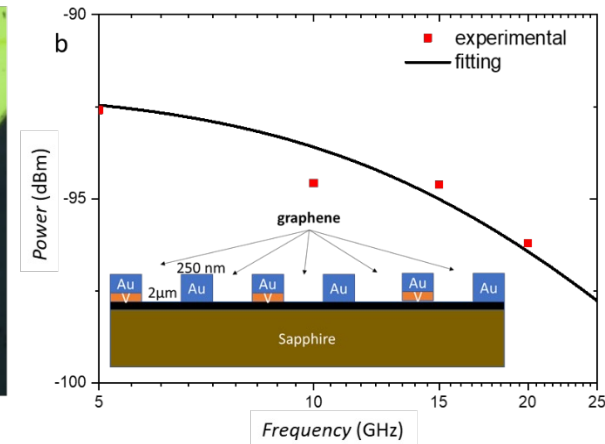
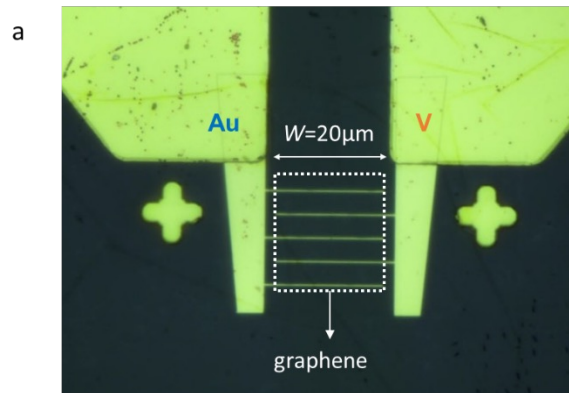
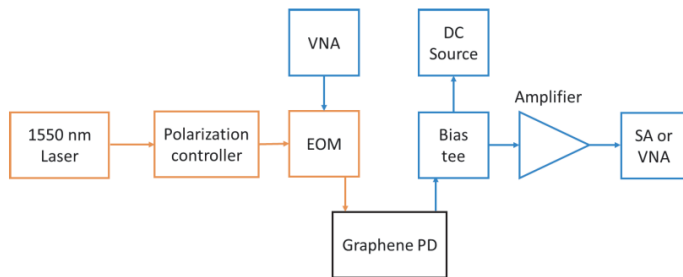
Photoresponse measurements



Ultrafast photodetectors based on graphene

Main characteristics of graphene photodetectors:

- ✓ Bandwidth: **>17 GHz**
- ✓ Signal/noise ratio: **45 dB**



- We have demonstrated that a two-terminal device based on CVD graphene can be used as a THz radiation mixer with a **5.8 GHz bandwidth** and $\text{NEP} = 1 \text{ nW/Hz}^{0.5}$.
- We have demonstrated that a two-terminal device based on graphene can be used as photodetectors at telecom wavelength with **20 GHz bandwidth**.



P. An, V. Kovalyuk, P. Bondareva, N. Kaurova, G. N. Goltsman, *Moscow Pedagogical State University*



G. Fedorov , M. Moskotin *Moscow Institute of Physics and Technology*



V. Ryzhii⁴ , T Otsuji, *RIEC, Japan*



E.D. Obraztsova, M. Rybin, **Prokhorov General Physics Institute, Moscow, Russia**

Thank you for attention!!!